Supporting Information

Selective Photocatalytic CO_2 Reduction in Water by Electrostatic Assembly of CdS Nanocrystals with a Dinuclear Cobalt Catalyst

Qian-Qian Bi, † *Jia-Wei Wang,* † *Jia-Xin Lv, Juan Wang, Wen Zhang,** and *Tong-Bu Lu**

Institute for New Energy Materials and Low Carbon Technologies, School of Materials Science and Engineering, Tianjin University of Technology, Tianjin 300384, China.

Corresponding Author

* E-mail: zhangwen@email.tjut.edu.cn.

* E-mail: lutongbu@mail.sysu.edu.cn.

Instrumentation and Methods

All solvents and reagents were commercially available and used without further purification, unless otherwise noted. All experiments were performed in deionized water at 25 °C. NMR spectra were recorded on Bruker 400 MHz instrument in D_2O, and chemical shifts were recorded in parts per million (ppm). High resolution mass spectra were performed on Q-TOF LC-MS with an ESI mode. UV−vis diffused reflectance spectra were carried out on a Lambda 750 UV/vis/NIR spectrophotometer. Raman spectrum was recorded on a high-resolution laser confocal fiber Raman

spectrometer (HORIBA EVOLVTION, HORIBA Jobinyvon, France). XPS (X-ray photo-electron spectroscopy) was detected with Al Kα as the excitation source on an ESCALAB 250 Xi spectrometer (Thermo Scientific, America). TEM (Transmission electron microscope) and high-resolution TEM (HRTEM) images were performed on Talos F200X, FEI, America using 200 kV acceleration voltage. Photoluminescence (PL) spectra were detected by a fluorescence spectrophotomer (F-7000, Hitachi, Tokyo, Japan). The time-resolved fluorescence measurements were measured by time-resolved confocal fluorescence instrument (MicroTime 200, PicoQuant, Berlin, Germany). Mott−Schottky plots were determined by impedance-potential technique using a three-electrode system, FTO (10 Ω sq^{-1}) with a geometrical area of 1.0 × 2.5 cm^2 , Ag/AgCl (in 3 M KCl) and platinum plate (1.0 × 1.0 cm^2) as the working electrode, reference electrode and counter electrode, respectively.

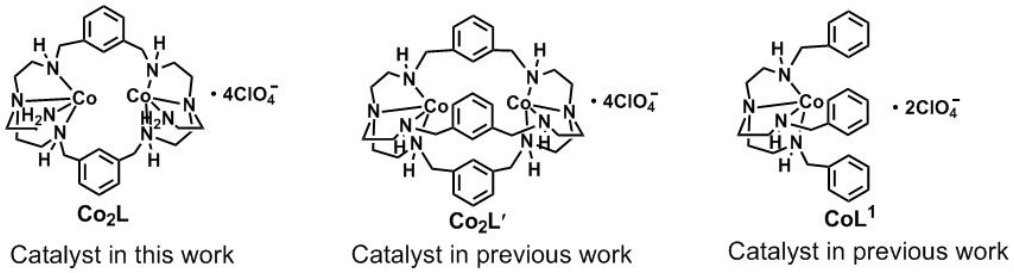

Figure S1. The structures of **Co_2L, Co_2L'**, and **CoL^1**.

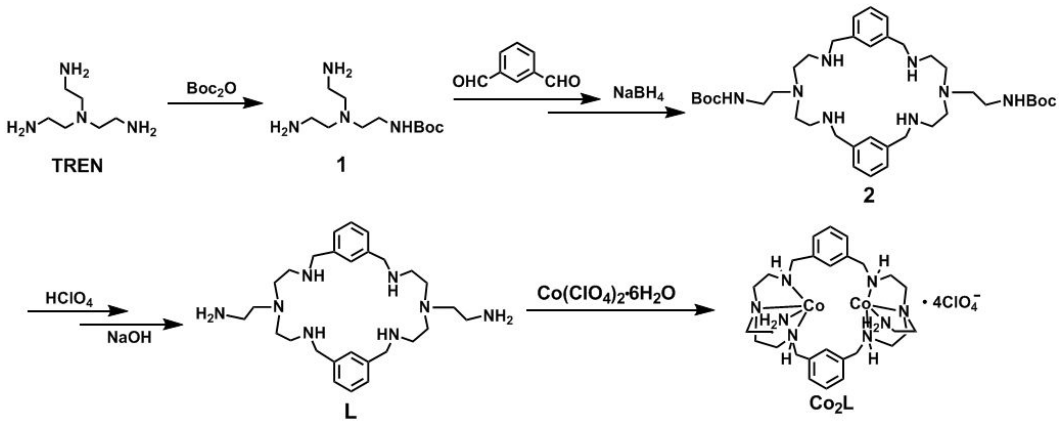

Scheme S1. Synthesis rout of Co_2L

Synthesis of dinuclear cobalt catalyst Co_2L

To a stirred solution of tris-(2-aminoethyl)amine (TREN) (5.1 mL, 35 mmol) in dioxane (30 mL) under nitrogen a solution of di-tert-butyl-dicarbonate (1.2 mL, 5.5 mmol) in dioxane (30 mL) was added over 1 h at rt. The reaction mixture was stirred for 17 h. The solvent was removed in vacuo and the residue was dissolved in water (10 mL). The aqueous solution was extracted with dichloromethane (6×15 mL). The organic phases were combined. The removal of the solvent in vacuo gave the product **1**. The product was purified by the silica gel column using CH_2Cl_2/MeOH/$NH_3 \cdot H_2O$ as an eluent. The volume ratio of the mixed eluent gradually increased from 1:1:0 to 0:8:1. R_f = 0.26 (DCM:MeOH:$NH_3 \cdot H_2O$=0:6:1). The product **1** was obtained as a viscous oil (1.247 g, 92%).

The product **1** (0.85 g, 3.45 mmol) was dissolved in 30 mL of MeOH. Under stirring, a solution of 1,3-benzenedialdehyde (0.46 g, 3.45 mmol) in MeOH (150 mL) was added dropwise over 3 h at room temperature. After stirring for 20 h, the solution was heated to 50 °C and hydrogenated with $NaBH_4$ (2.76 g, 34.5 mmol). When the addition was complete, the reaction mixture was stirred at 50 °C overnight. The solvent was then removed and the residue was dissolved in basic water (20 mL, pH = 9), and extracted with 15 mL of CH_2Cl_2 (×5). The collected organic phase was dried over Na_2SO_4. After evaporation of the solvent, the product **2** was obtained as a white solid (yield, 80%). The product was deprotected with $HClO_4$ (8.5 mL, 149 mmol) in MeOH for 12h. After filtration and neutralization, the residue of **L** was used directly to the next step. For **1**, ^{1}H NMR (400 MHz, $CDCl_3$) δ 5.54 (s, 1H), 3.23-3.12 (m, 2H),

2.88-2.74 (m, 4H), 2.72-2.43 (m, 10H), 1.44 (s, 9H). ^{13}C NMR (100 MHz, $CDCl_3$) δ 156.40, 79.03, 55.56, 54.26, 39.08, 38.74, 28.48. HRMS (ESI) *m*/*z* $[M + H^+]^+$ Anal. calcd for $C_{11}H_{27}N_4O_2^+$ 247.2134, found 247.2183 For **L**, ^{1}H NMR (400 MHz, D_2O) δ 7.60-7.54 (m, 8H), 4.29 (s, 8H), 3.24 (t, J = 6.3 Hz, 8H), 3.16 (t, J = 6.5 Hz, 4H), 2.93-2.89 (m, 12H). ^{13}C NMR (100 MHz, D_2O) δ 131.80, 131.20, 131.14, 130.25, 50.90, 49.76, 48.57, 43.97, 35.93. HRMS (ESI) *m*/*z* $[M + 2HClO_4 + H^+]^+$ Anal. calcd for $C_{28}H_{51}Cl_2N_8O_8^+$ 697.3207, found 697.5135.

Under an argon atmosphere, an anhydrous ethanol solution (12 mL) of $Co(ClO_4)_2 \cdot 6H_2O$ (2.07 g, 5.67 mmol) was added to an anhydrous ethanol solution (250 mL) containing $L \cdot 8HClO_4$ (3.00 g, 2.14 mmol) and NaOH (0.67 g, 16.80 mmol). The mixture was stirred at room temperature for 2 h. The resulted brown precipitate was filtered, washed with ethanol and diethyl ether, and dried under vacuum to give a brown powder Co_2L (1.74 g, 75%). ESI-MS (CH_3CN, Ar atmosphere): m/z calcd for **Co_2L** HRMS (ESI) *m*/*z* $[M + OH^- + HCOO^-]^{2+}$ Anal. calcd for $C_{29}H_{50}N_8Co_2O_3$ 338.1335. Found: 338.3450.

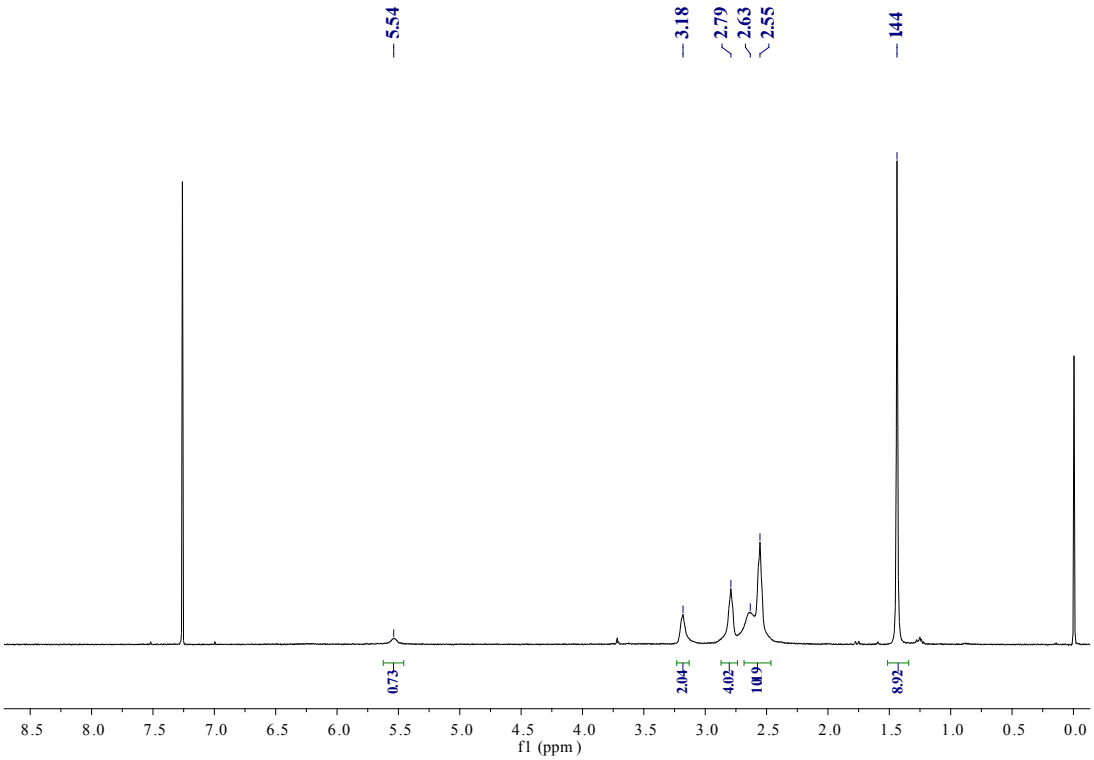

Figure S2. ^{1}H NMR spectrum of **1** ($CDCl_3$, 400 MHz, 25 °C).

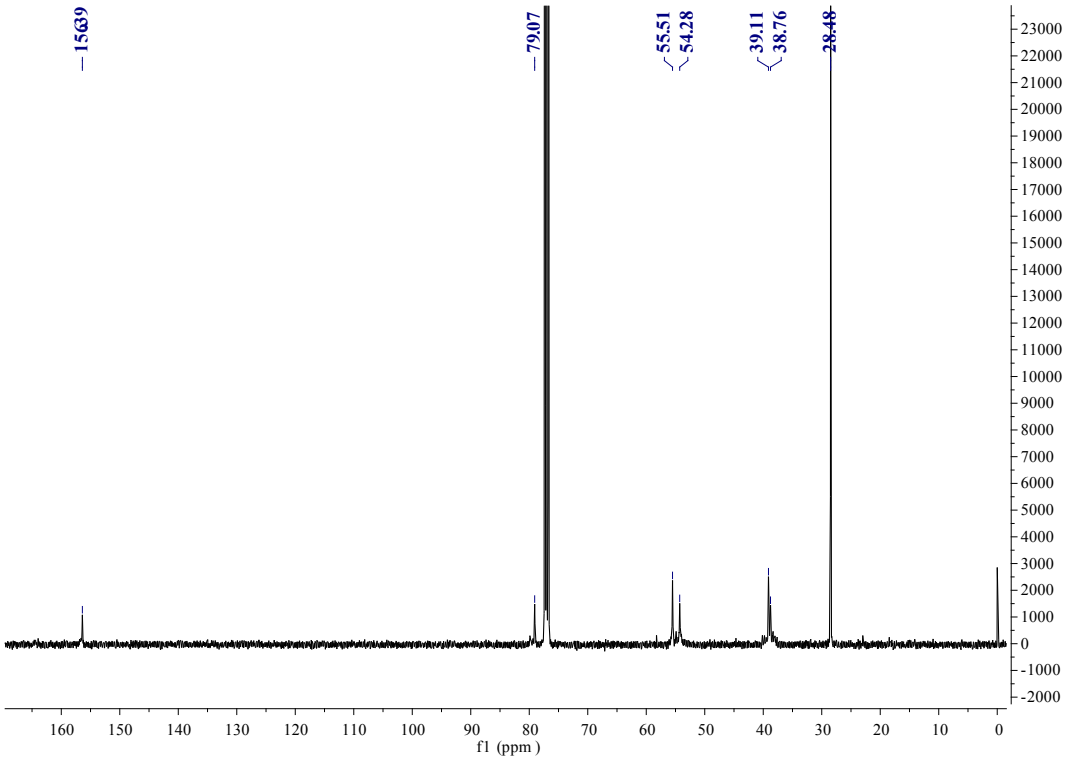

Figure S3. ^{13}C NMR spectrum of **1** ($CDCl_3$, 100 MHz, 25 °C).

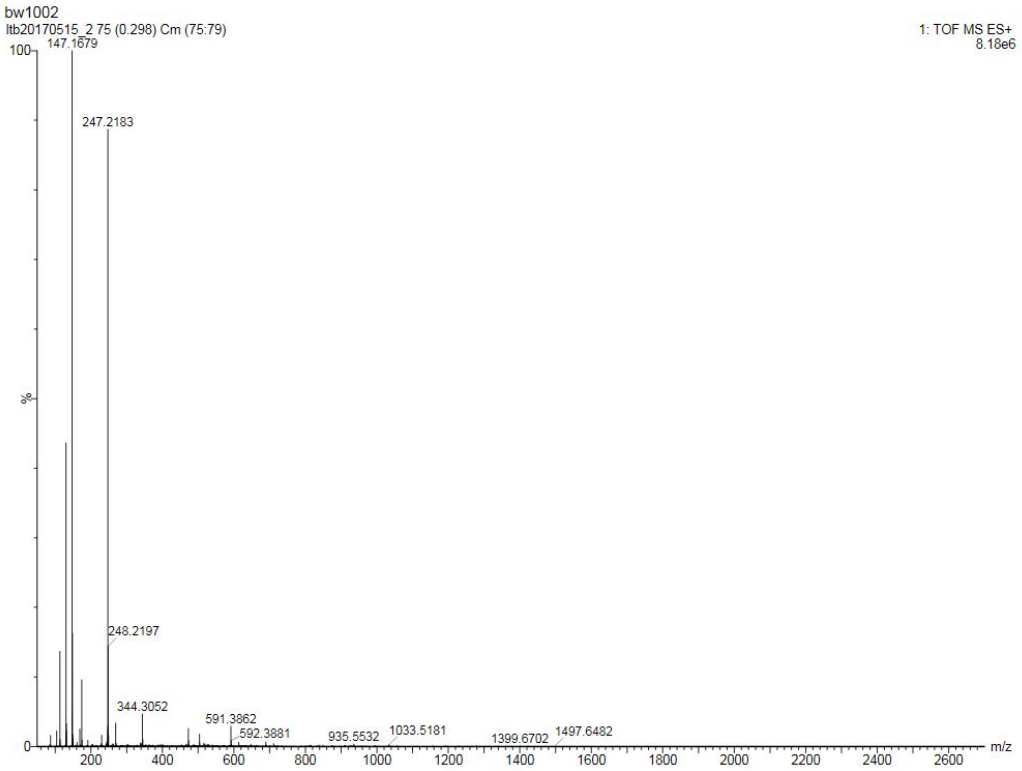

Figure S4. HRMS (ESI) spectrum of **1**.

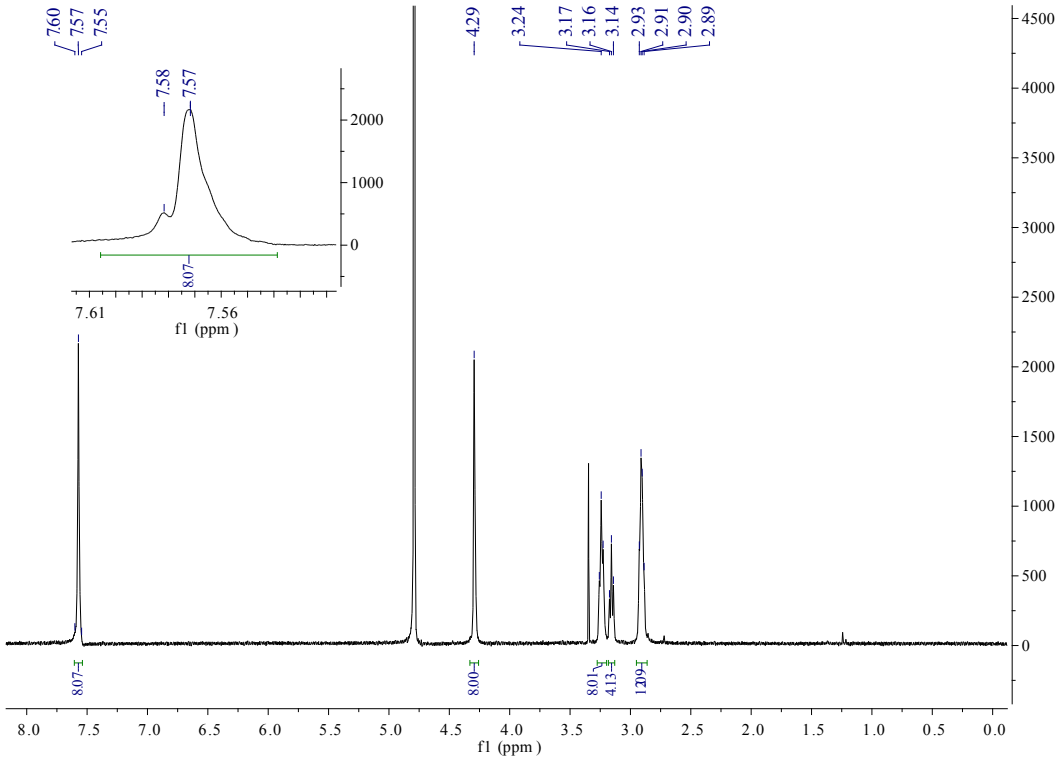

Figure S5. ^{1}H NMR spectrum of L (D_2O, 400 MHz, 25 °C).

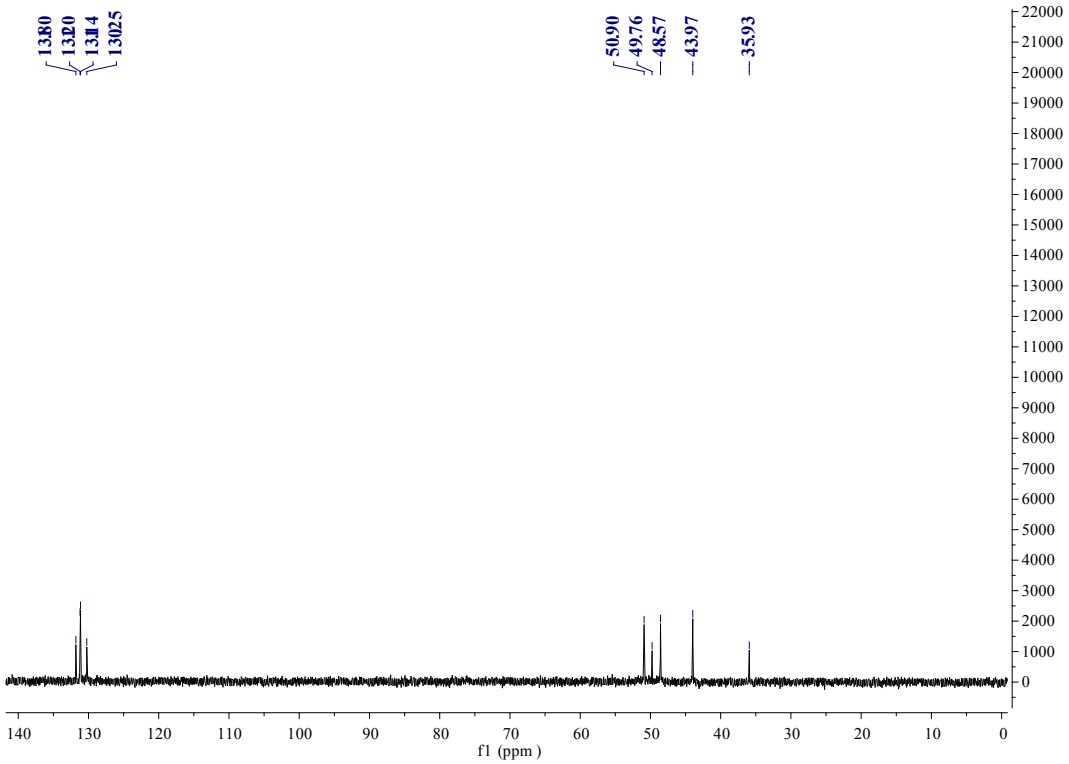

Figure S6. ^{13}C NMR spectrum of L (D_2O, 100 MHz, 25 °C).

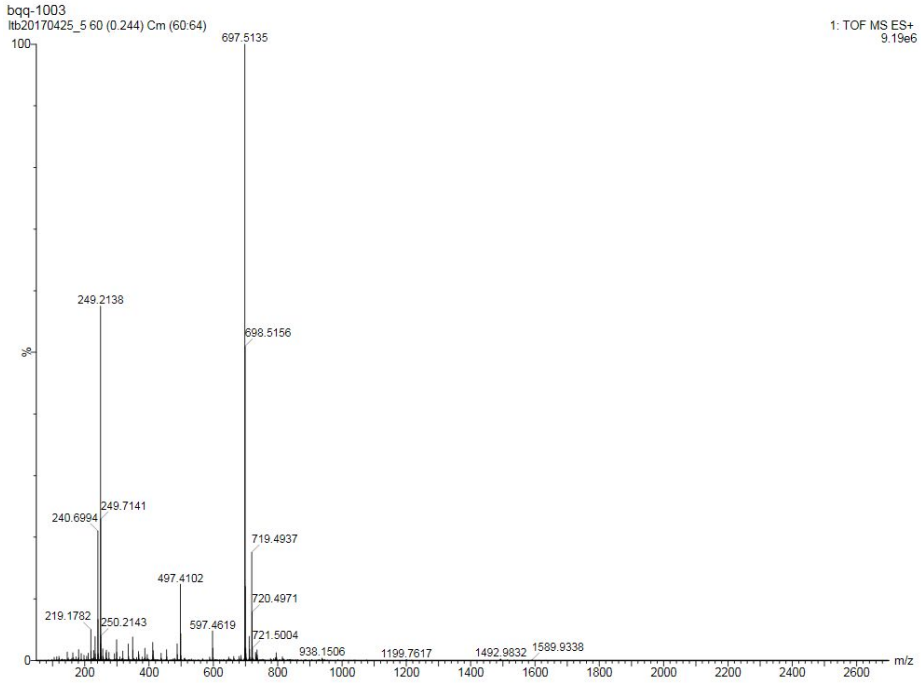

Figure S7. HRMS (ESI) spectrum of L.

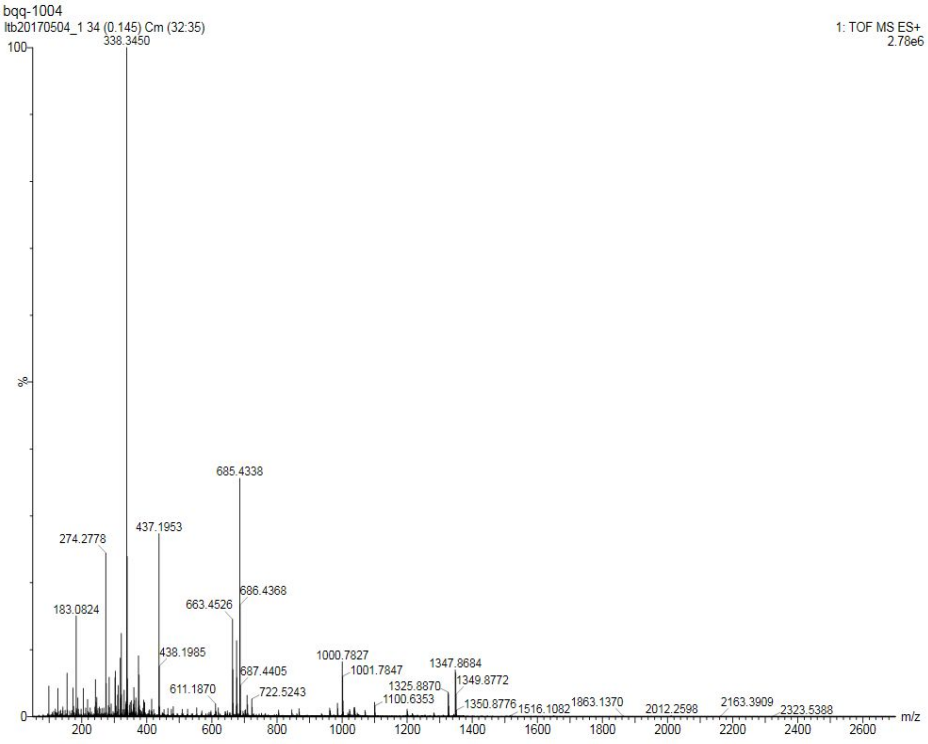

Figure S8. HRMS (ESI) spectrum of Co_2L.

Synthesis of CdS NCs

CdS NCs with different surface functionalities were prepared by ligand exchange (CdS-MPA) or ligand stripping (CdS-BF_4) of oleic acid-capped NCs (CdS-OA) as previously reported.

CdS-OA. The CdS-OA was synthesized according to the reported literature. Under argon atmosphere, a solution of CdO (0.64 g, 4.21 mmol) and OA (26 g, 92 mmol) in ODE (70 g, 237 mmol) were heated to 285 ℃. A solution of sulfur (0.08 g, 2.5 mmol) in ODE (30 g, 120 mmol) was instantly added to the above system. Then the mixture solution was cooled to 250 ℃ and remained for 120 s before rapidly cooled to room temperature by an ice bath. The nanoparticles were precipitated from mixture solution using methanol/hexane (1:1) and excess acetone, obtained by centrifugation at 7000 rpm at 3 min and re-dissolved in hexane. Before finally dispersing in hexane,

extraction process was performed by twice using hexane and excess acetone as solvent and non-solvent, respectively, before the final dispersion in hexane.

CdS-MPA. Ligand exchange with MPA was prepared according to a reported procedure. MPA (0.5 mL) was dispersed in chloroform/methanol (1:1, 10 mL) and the pH adjusted to 10.5 with TMAOH. CdS-OA solution (2 mL) was added to this mixture and stirred in the dark for 2 d. The NCs were precipitated with excess acetone and centrifuged (7000 rpm, 3 min). The isolated particles were washed with acetone before being dispersed in water (1 mL).

CdS-MPAH. CdS-MPAH was prepared by the protonation of **CdS-MPA,** that is **CdS-MPA** was dissolved in ultrapure water, then the pH of the aqueous solution were adjust to 6, 5, 4 by HCl solution, respectively. The protonation of CdS-MPA was characterized by zeta potential experiments.

CdS-BF_4. Ligand-free particles were carried out by a reported procedure. CdS-OA solution (2 mL in hexane) was reduced to dryness and re-dispersed in a mixture of anhydrous $CHCl_3$ (6 mL) and anhydrous DMF (0.4 mL). Under nitrogen atmosphere, triethyloxonium tetrafluoroborate solution (8 mL) was added and stirred for 1 h. Aliquots of trimethyloxonium tetrafluoroborate solution (1.0 M in CH_3CN) were added until the particles precipitated. The stripped particles were centrifuged (7000 rpm, 3 min), dried in air for 1 min, and re-dispersed in DMF (2 mL).

CdS concentration determination. The concentration of CdS (in moles of particles) was estimated from the UV absorption spectrum using the method developed by Peng and co-workers. The average particle diameter, *D*, was determined from the

wavelength of the first absorption maximum, λ, and the concentration of particles was determined from the absorbance at the wavelength of the first absorption maximum using the Beer-Lambert law, and an extinction coefficient, ϵ. A and A_m are the calibrated absorbance and the measured absorbance, respectively. $(hwhm)_{UV}$ is the half width at the half-maximum on the long wavelength side of the first absorption peak. K is the average $(hwhm)_{UV}$ of the standard samples used for the measurements. For CdS nanocrystals, the average $(hwhm)_{UV}$ values of the standard samples are 11.

$$D = (-6.6521 \times 10^{-8})\lambda^3 + (1.9557 \times 10^{-4})\lambda^2 - (9.2352 \times 10^{-2})\lambda + (13.29)$$

$$\epsilon = 21536\ (D)^{2.5}$$

$$A = A_m\ (hwhm)_{UV}/K$$

$$A = \epsilon CL$$

Electrochemical experiments. Electrochemical experiments were performed with an electrochemical workstation (CHI 760E). Mott–Schottky plots of CdS-MPA (4 μM) in aqueous solution containing 0.5 M Na_2SO_4 at 25 ˚C were generated with impedance-potential technique, using a three-electrode system with a glassy carbon electrode (0.07 cm^2) , a platinum plate (1.0 cm^2) and silver–silver chloride (Ag/AgCl, in 3 M KCl) as the working ,the counter and reference electrodes, respectively. The capacitance of the semiconductor–electrolyte interface was collected at 1 kHz, with 10 mV AC voltage amplitude. CV curves of Co_2L (0.5 mM) were completed using a glassy carbon working electrode (0.07 cm^2), a Pt wire auxiliary electrode, and an Ag/AgCl (3 M KCl) reference electrode in 0.1 M KCl aqueous solution at 25 ºC. The

electrolyte solution was saturated by bubbling with Ar or CO_2 for 30 min prior to each experiment.

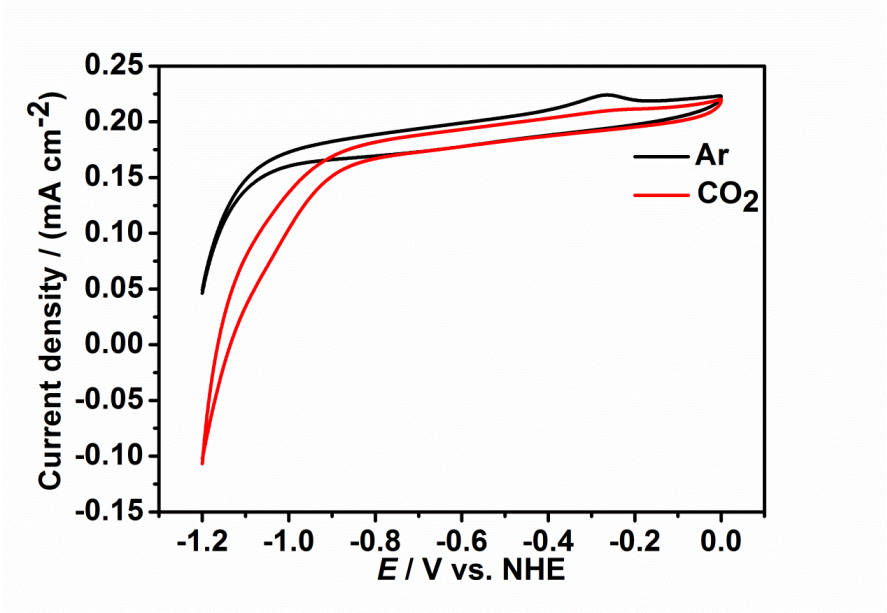

Figure S9. CV curves of 0.5 mM Co_2L in aqueous solution containing 0.1 M $NaHCO_3$ under an Ar (black) and CO_2 atmosphere (red) at 25 °C, using a glassy carbon electrode with a scan rate of 100 $mV \cdot s^{-1}$

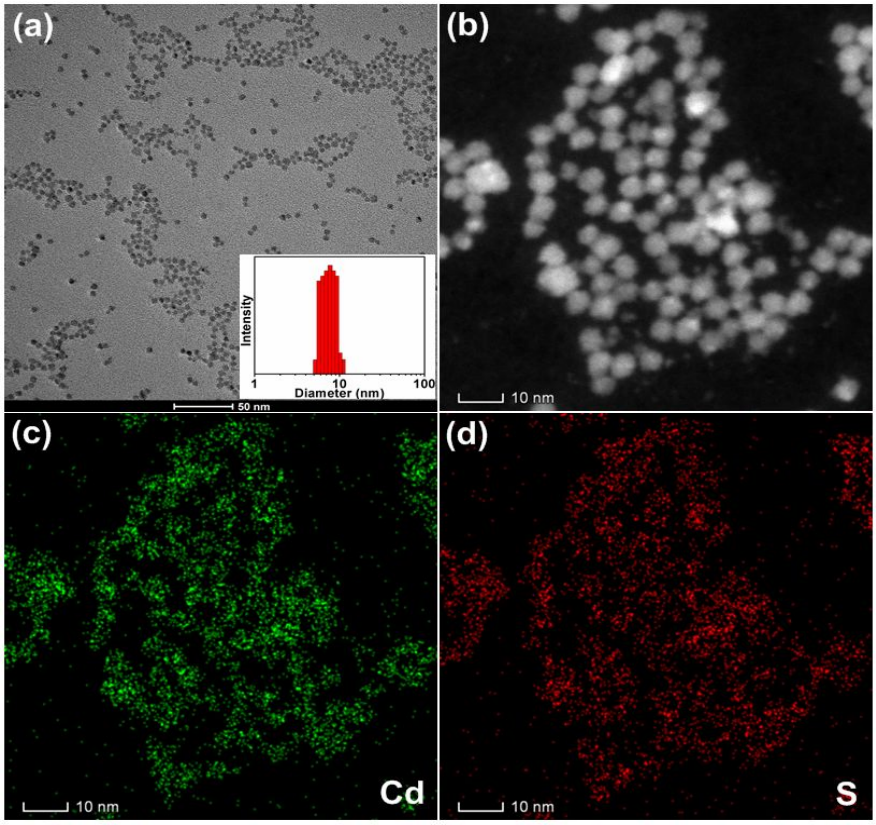

Figure S10. (a) TEM images of CdS-MPA (inset: DLS data); (b, c, d) The HADDF image for CdS-MPA and elemental mapping of the selected part.

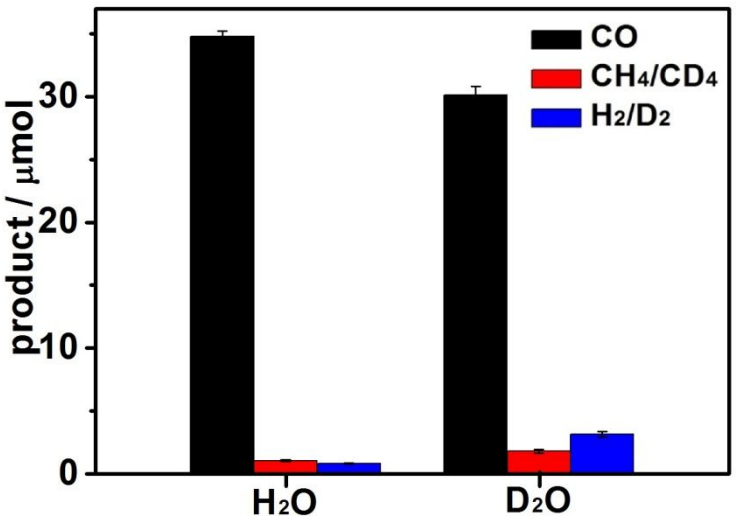

Figure S11. CO_2 photoreduction results using H_2O (a) and D_2O (b) with CdS-MPA (4 μM), Co_2L (1 μM), under TEOA (0.3 M), 25 mL of 0.1 M $NaHCO_3$ aqueous solution, 300 W Xe lamp ($\lambda > 420$ nm).

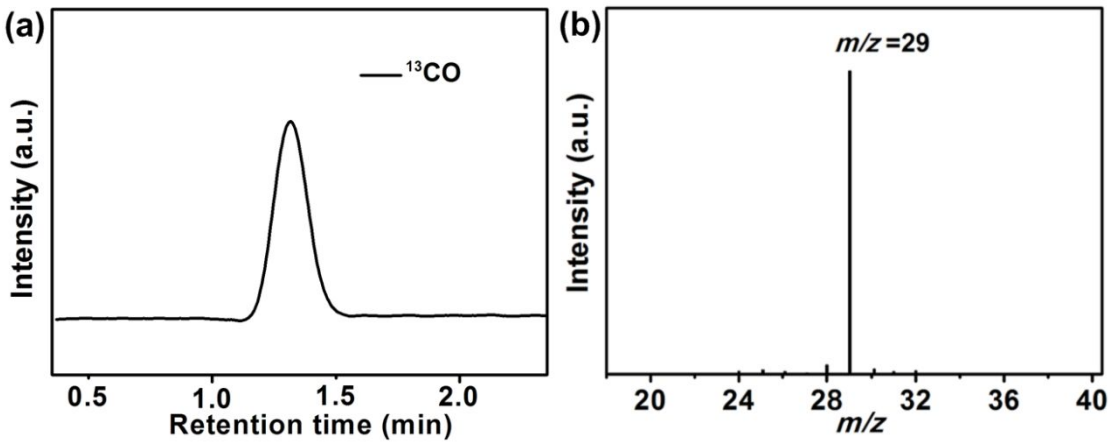

Figure S12. Gas chromatogram and mass spectra (GC-MS) analysis for the gas generated from the photocatalytic reduction of $^{13}CO_2$. (a) Gas chromatogram, t = 1.26 min corresponds to the retention time of ^{13}CO. (b) Mass spectra, *m*/*z* = 29 corresponds to the formula weight of ^{13}CO.

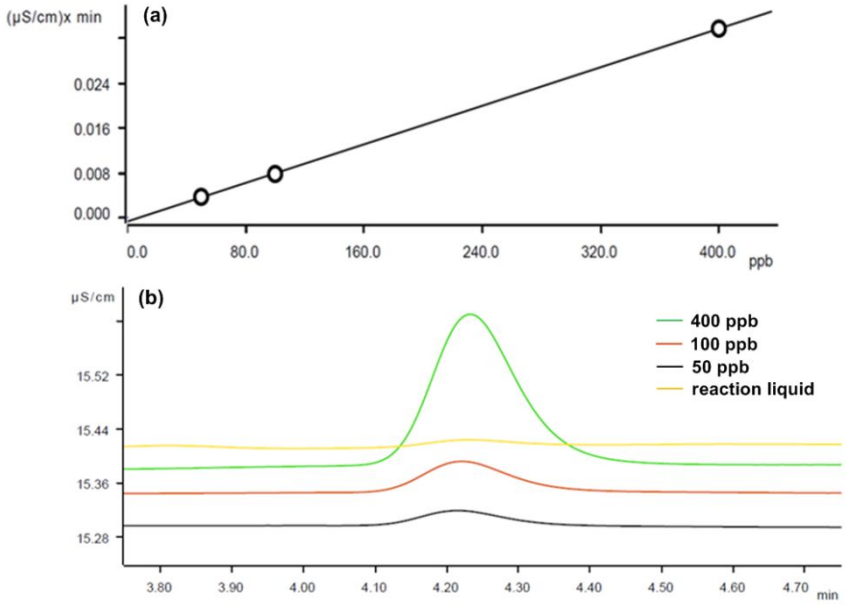

Figure S13. (a) The standard curve of formate, and (b) the ion chromatogram of the reaction liquid, indicating the amount of formed formate is negligible (about 1.8 ppb).

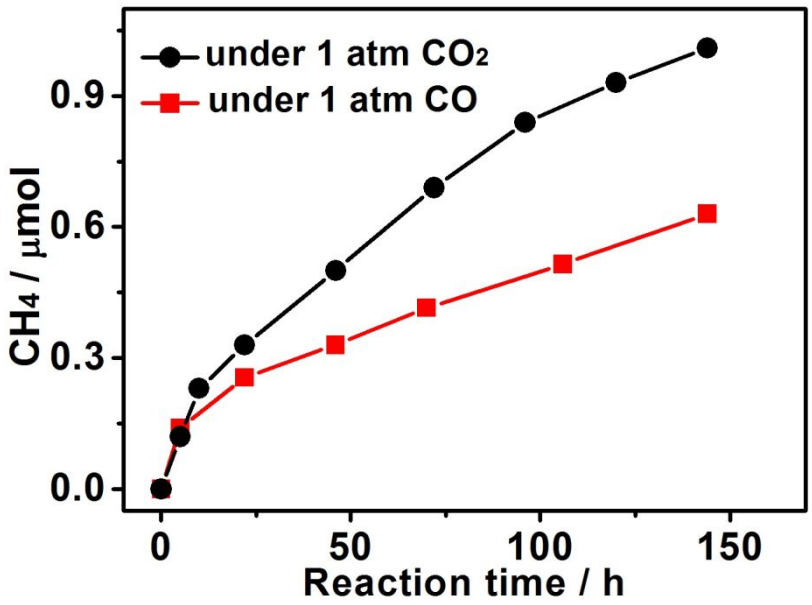

Figure S14. The evolution of CH_4 under CO_2 (black) and CO (red) atmosphere catalyzed by CdS-MPA/Co_2L.

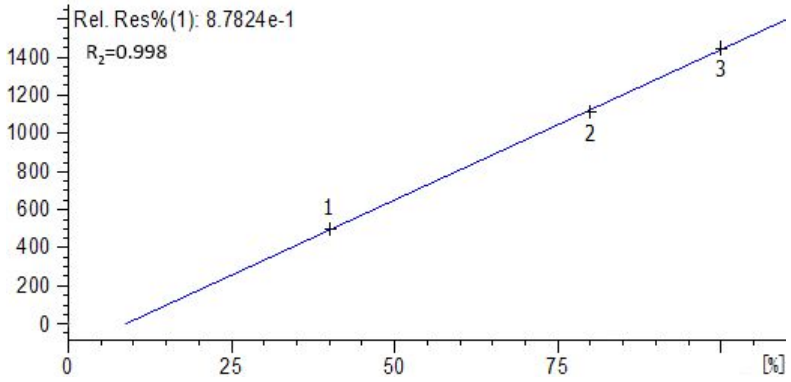

Figure S15. The standard curve of CO_2.

Table S1. The carbon balance result during the photoreaction.

	CO_2 / μmol	CO /μmol	CH_4 / μmol	HCOOH / μmol
Before reaction	2097.74	0	0	0
After reaction	2059.57	34.51	1.01	0.1

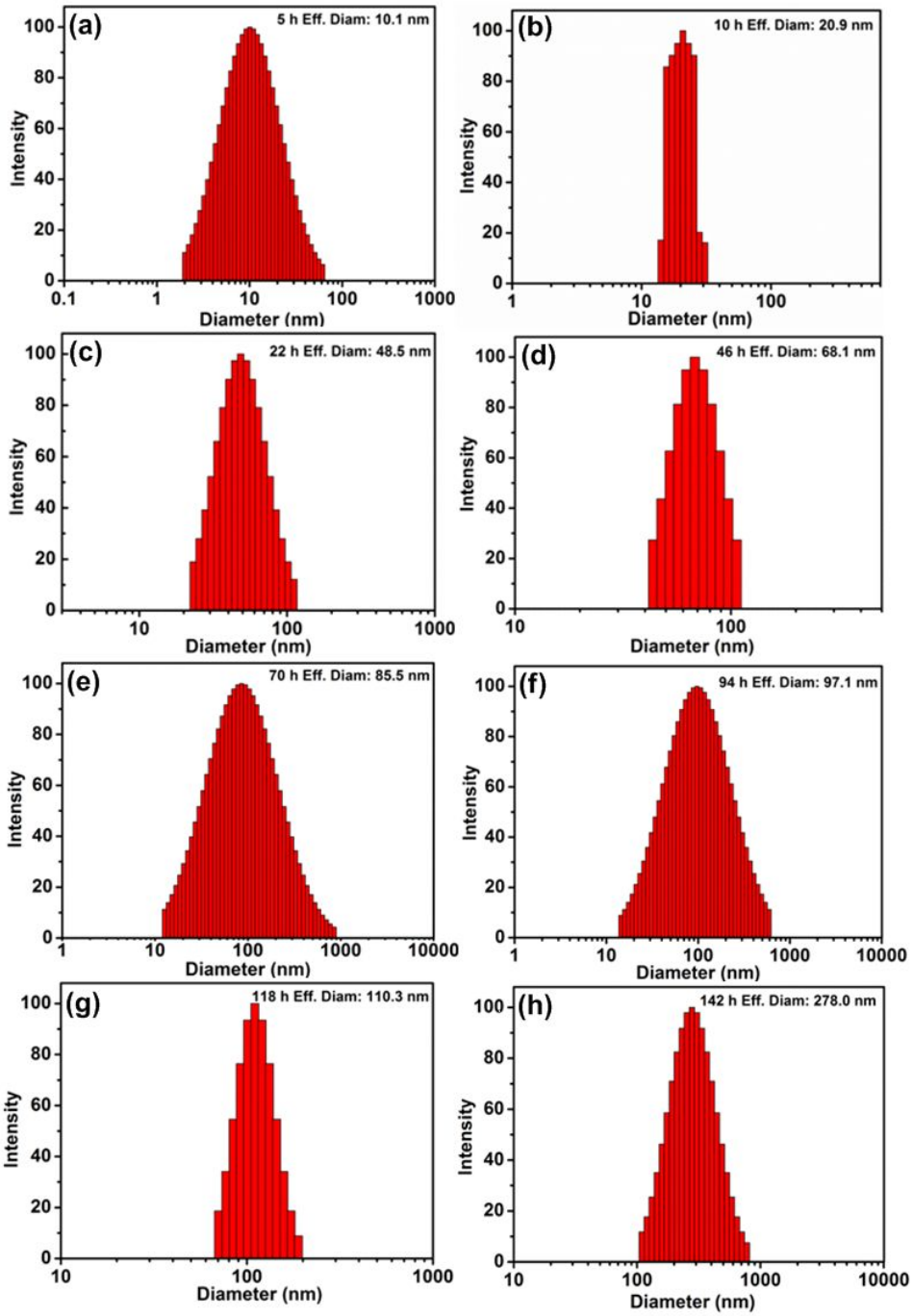

Figure S16. DLS of CdS-MPA at different reaction time.

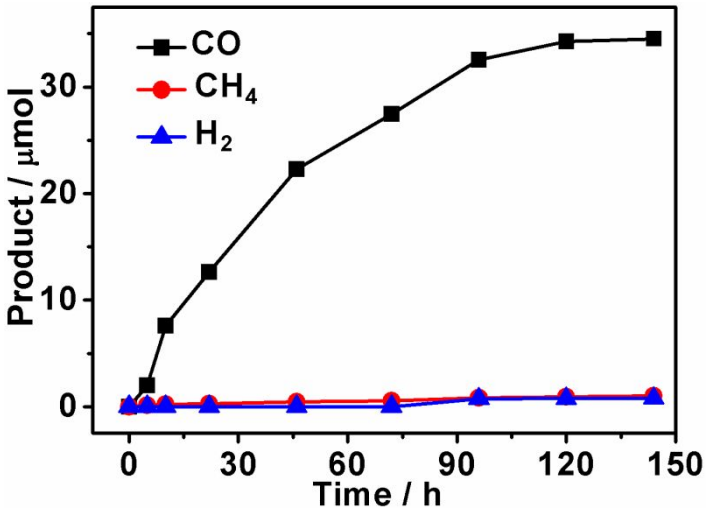

Figure S17. Photocatalytic evolution of CO (black), CH_4 (red) and H_2 (blue) catalyzed by CdS-MPA (4 μM) and Co_2L (1 μM) in a 25 mL of 0.1 M $NaHCO_3$ aqueous solution containing 0.3 M TEOA, irradiated with 300 W Xe lamp (λ > 420 nm).

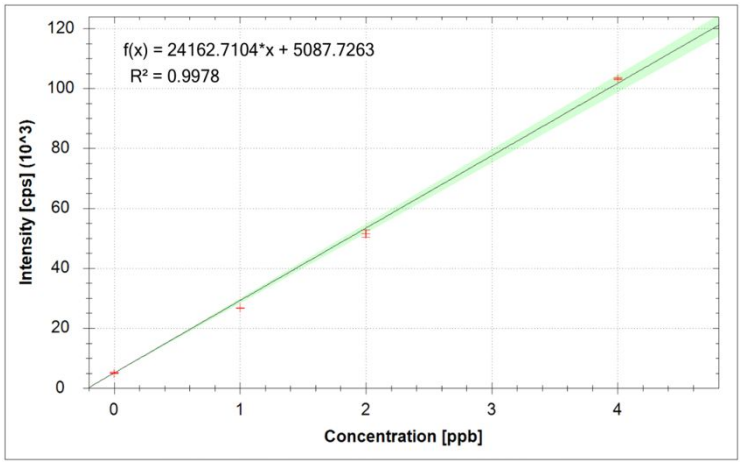

Figure S18. Standard curves of pure Co^{2+} for ICP-MS measurements, the amount of Co^{2+} in CdS-MPA@Co_2L was calculated as follow: 2.5 mg isolated solid from the centrifugation of the reaction mixture was dissolved into 5 mL concentrated HNO_3 and diluted to 1666.66 mL in which the concentration of the sample was 1500 ppb. According to the formula of f(x) = 24162.7104*x + 5087.7263, the concentration of Co^{2+} was measured as 0.796 ppb, thus, the mass fraction of Co^{2+} was calculated as 0.053 ± 0.005%.

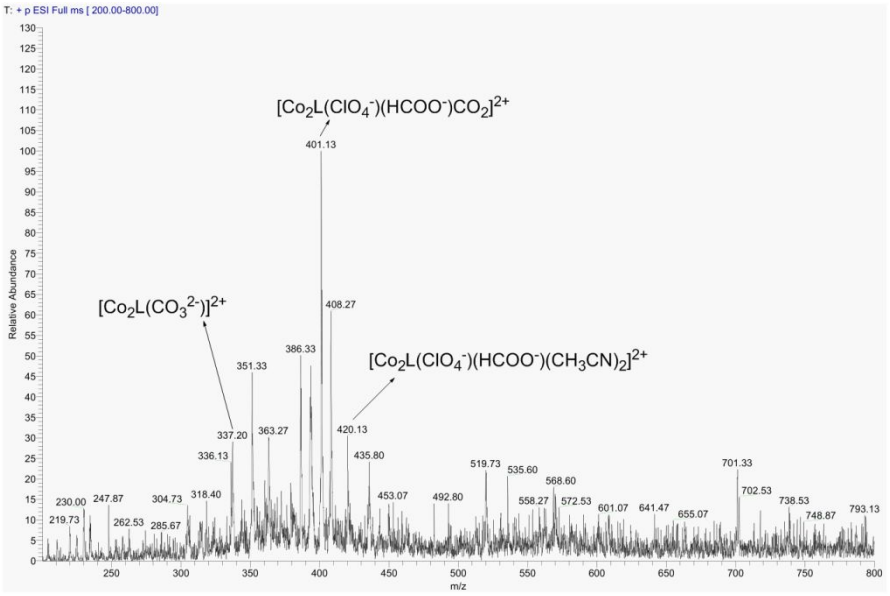

Figure S19. LC-MS (ESI) of the isolated solid from the centrifugation of the reaction mixture after ultrasound for 5 h in CH_3CN solution. m/z = 401.13 $[Co_2L(ClO_4^-)(HCOO^-)CO_2]^{2+}$, m/z = 337.20 $[Co_2L(CO_3^{2-})]^{2+}$, m/z = 420.13 $[Co_2L(ClO_4^-)(HCOO^-)(CH_3CN)_2]^{2+}$.

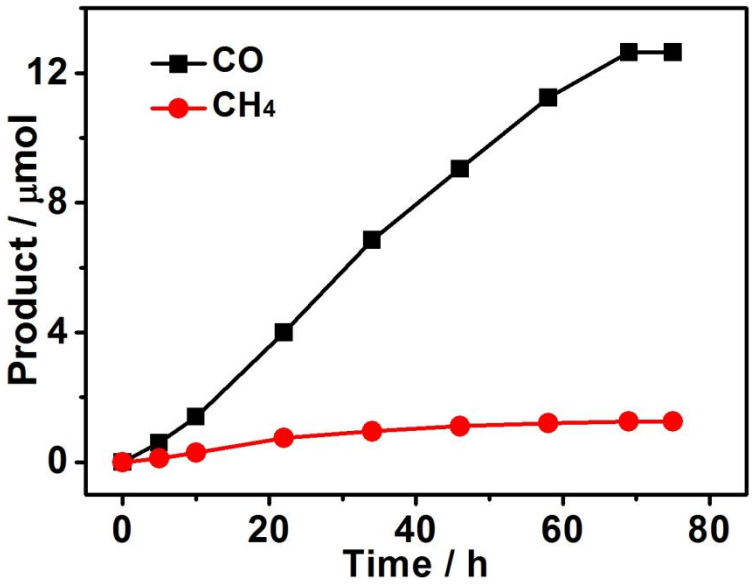

Figure S20. CO_2 photoreduction results using the isolated CdS-MPA/Co_2L after the first run of photocatalytic reaction.

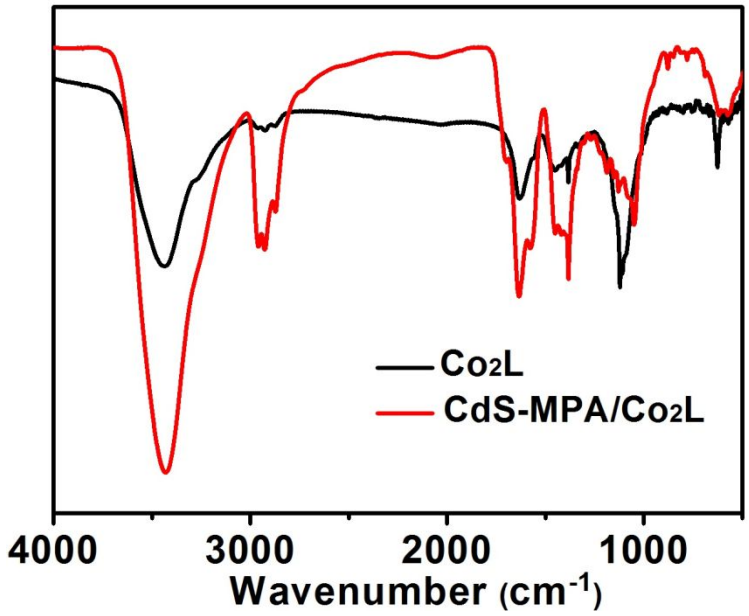

Figure S21. IR spectra of Co_2L (black line) and CdS-MPA/Co_2L after photoreaction (red line).

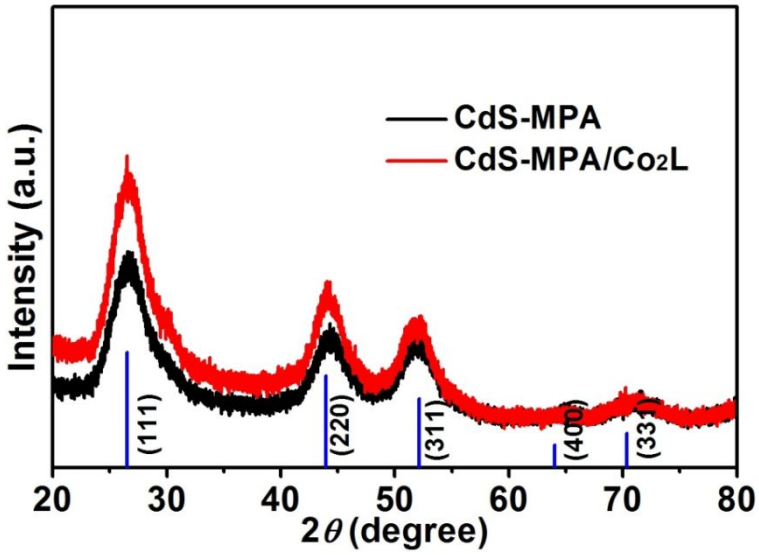

Figure S22. XRD patterns of CdS-MPA before reaction (black line) and CdS-MPA/Co_2L after reaction (red line), both showing the cubic phase structure of CdS nanocrystals (JCPDS 80-0019).

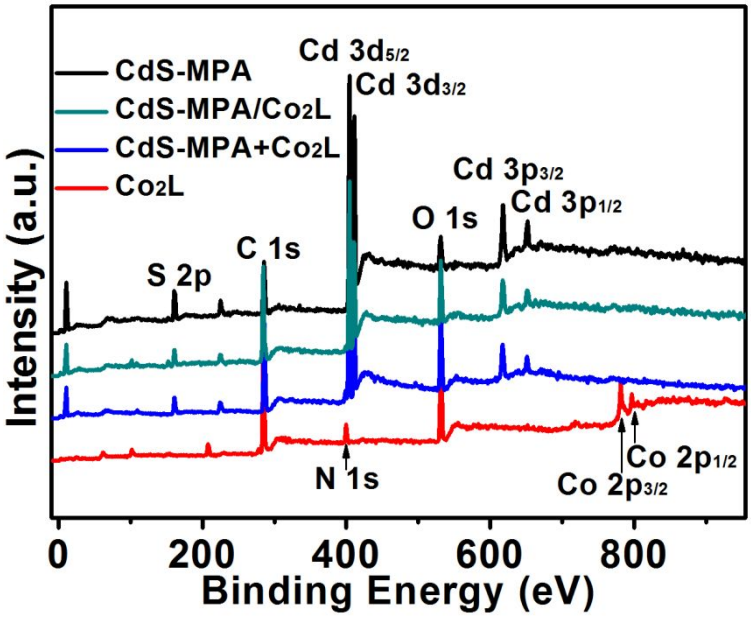

Figure S23. XPS scans of CdS-MPA (black line), the isolated CdS-MPA/Co_2L solid after CO_2 reduction (green line), the mixture of CdS-MPA and Co_2L before CO_2 reduction (blue line) and Co_2L (red line).

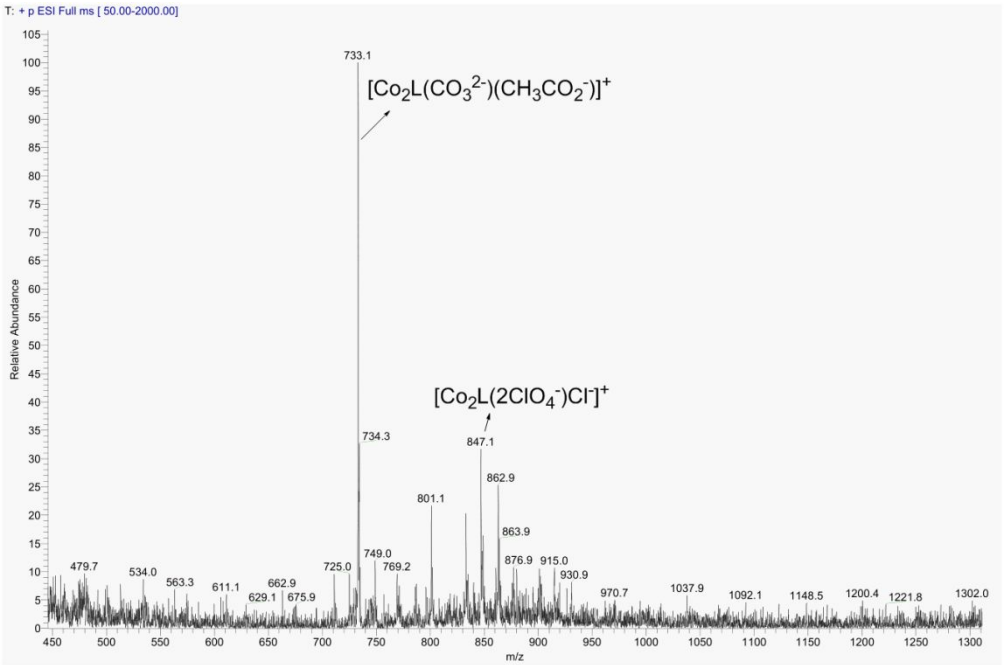

Figure S24. ESI-MS results of the supernatant from the photoreaction mixture with 280 μM Co_2L. Signals: m/z = 733.1 for $[Co_2L(CO_3^{2-})(H_3COO^-)]^+$, m/z = 847.1 for $[Co_2L(ClO_4^-)_2Cl^-]^+$.

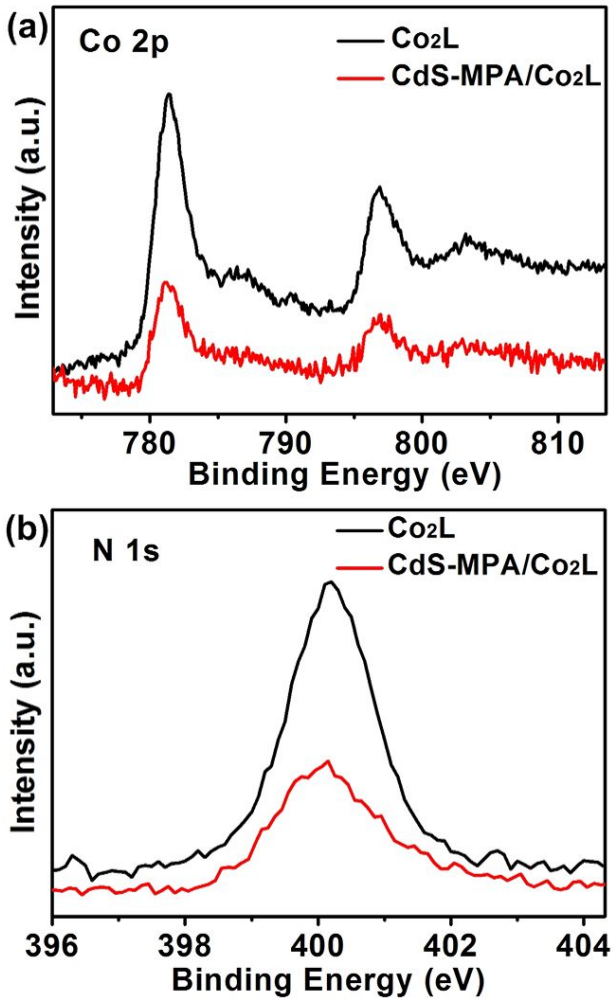

Figure S25. XPS spectra of Co_2L and CdS-MPA/Co_2L. (a) Co 2p spectrum. (b) N 1s spectrum.

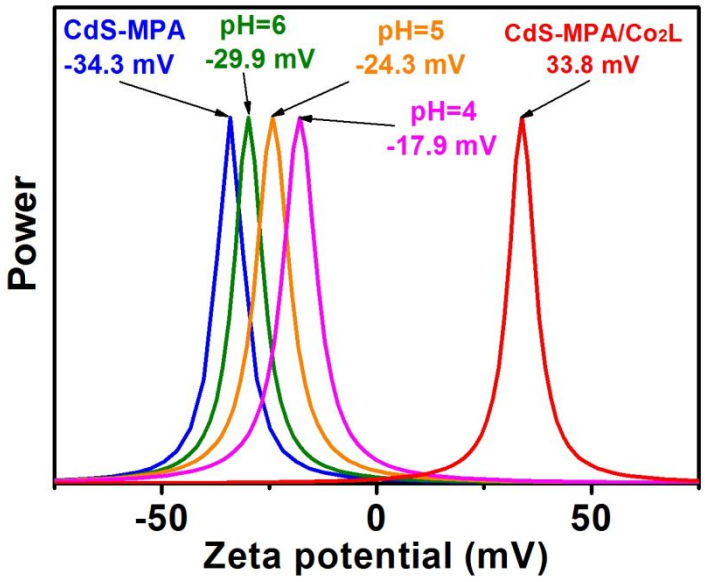

Figure S26. Zeta potentials of CdS-MPAH at pH 6, 5 and 4.

Table S2. A Comparison of the Reported Photocatalytic CO_2 Reductions Using Noble Metal Free Catalysts.

Catalyst	Solvent	Solvent volume /mL	Amount of catalyst	Product (μmol)	TON	Sel.	Ref.
CdS-MPA /Co_2L	0.1 M $NaHCO_3$ in H_2O	25	2.5×10^{-8} mol	34.5 μmol CO	1380	95%	This work
CdS /[Ni(terpy)$_2$]	H_2O	2	2.0×10^{-7} mol	4.0 μmol CO	20	90%	1
$CuInS_2$ /ZnS/FeTPP	DMSO	415	8.3×10^{-7} mol	0.05 μmol CO	60	84%	2
$CuInS_2$ /ZnS/FeTMA	5 mM KCl in H_2O	5	5.0×10^{-9} mol	0.22 μmol CO	450	99%	3
$Zn_{0.14}Cd_{0.84}S$/ FeTCPP	CH_3CN /H_2O(3/1)	100	1.4×10^{-5} mol	1.28 μmol CO	9.2	93%	4
g-C_3N_4 /FeTCPP	CH_3CN /H_2O(3/1)	100	1.1×10^{-7} mol	~0.60 μmol CO	~6.0	98%	5

Reference

(1) Kuehnel, M. F.; Orchard, K. L.; Dalle, K. E.; Reisner, E. Selective Photocatalytic CO_2 Reduction in Water through Anchoring of a Molecular Ni Catalyst on CdS Nanocrystals. *J. Am. Chem. Soc.* **2017,** *139*, 7217-7223.

(2) Lian, S.; Kodaimati, M. S.; Dolzhnikov, D. S.; Calzada, R.; Weiss, E. A. Powering a CO_2 Reduction Catalyst with Visible Light through Multiple Sub-Picosecond Electron Transfers from a Quantum Dot. *J. Am. Chem. Soc.* **2017,** *139*, 8931-8938.

(3) Lian, S.; Kodaimati, M. S.; Weiss, E. A. Photocatalytically Active Superstructures

of Quantum Dots and Iron Porphyrins for Reduction of CO_2 to CO in Water. *ACS Nano* **2018,** *12*, 568-575.

(4) Li, P.; Zhang, X.; Hou, C.; Lin, L.; Chen, Y.; He, T. Visible-Light-Driven CO_2 Photoreduction over $ZnxCd_{1-X}S$ Solid Solution Coupling with Tetra(4-Carboxyphenyl)Porphyrin Iron(III) Chloride. *Phys. Chem. Chem. Phys.* **2018,** *20*, 16985-16991.

(5) Lin, L.; Hou, C.; Zhang, X.; Wang, Y.; Chen, Y.; He, T. Highly Efficient Visible-Light Driven Photocatalytic Reduction of CO_2 over g-C_3N_4 Nanosheets/Tetra(4-Carboxyphenyl)Porphyrin Iron(III) Chloride Heterogeneous Catalysts. *Appl. Catal., B* **2018,** *221*, 312-319.